European Journal of Control xxx (xxxx) xxx

Contents lists available at ScienceDirect

European Journal of Control

journal homepage: www.elsevier.com/locate/ejcon

Prescribed–time estimation and output regulation of the linearized Schrödinger equation by backstepping

Drew Steeves[a,*], Miroslav Krstic[a], Rafael Vazquez[b]

[a] University of California San Diego, 9500 Gilman Dr., La Jolla, CA 92093, California
[b] Universidad de Sevilla, Avda. de los Descubrimientos, 41092 Seville, Spain

ARTICLE INFO

Article history:
Received 1 April 2019
Revised 19 February 2020
Accepted 26 February 2020
Available online xxx

Recommended by Prof. T. Parisini

Keywords:
Prescribed–time estimation
Output regulation
Backstepping
Distributed parameter systems

ABSTRACT

We study state estimation of the linearized Schrödinger equation within a prescribed terminal time. We make use of a time–varying, complex–valued observer gain and boundary measurements to construct the observer, where the gain is designed such that the estimate error converges to zero within the terminal time. The observer gain proposed herein is developed via the backstepping method by selecting a target error equation that stabilizes to zero within the terminal time. Our time–varying observer gain diverges as time approaches the terminal time. Nevertheless, we can guarantee prescribed–time stabilization of the estimator error equation by characterizing the growth–in–time of the observer gain and comparing it to the stability of the target error equation. We develop the full–state feedback dual result, and we combine the boundary estimation and control results to develop prescribed–time output regulation.

1. Introduction

We consider the problem of finite–time estimation and control of the linearized Schrödinger equation,

$$v_t(x,t) = -jv_{xx}(x,t), \tag{1}$$

by use of boundary measurements and actuation. Control and estimation problems for the linearized Schrödinger equation have received interest in the controls community in the past [4,22]. In these works, the guaranteed stabilization is of exponential type: the state or state estimate error are ensured to converge to zero at an exponential rate in time.

Our study differs from existing results in that we impose a more demanding type of stabilization: we require the quantities of interest to converge to zero within a finite time which is *prescribed independently of the initial conditions*. This type of stabilization, first introduced in [16] and later extended in [37], is a subclass of the predefined–, fixed–, and finite–time stabilization problems, which themselves are subclasses of asymptotic stabilization. Finite–time stability is when the attractivity property occurs within a bounded time which depends on the initial conditions [5,18,19,27,29]. Appearing later on in [3] is the stronger notion of fixed–time stability, where the convergence time admits a uniform upper bound (with respect to initial conditions). In particular, concerning fixed–time convergence: for a survey on sliding mode control, see [28], and for a related application (an exact differentiator), see [9]; for nonlinear feedback design using the block control and sliding mode approaches, see [26]; and for the implicit Lyapunov function approach, see [27].

The more recent notion of predefined–time stability requires attractivity to be achieved within a time $T_c := T_c(\rho)$ defined a priori independently of initial conditions but *depending on system parameters* ρ. Related to continuous deadbeat control (e.g., [34]), but having an autonomous system structure without delay terms, predefined–time convergence for some nonlinear systems can be established via a Lyapunov approach [20,21,33] and naturally extend to uncertain systems so long as T_c can be expressed by *known* parameters (see [21, Def. 2.5]).

Most of the aforementioned methods have yet to be extended for treating infinite–dimensional systems. The stability we establish for (1) eliminates any constraints on the bounded convergence time such that it is *prescribed* rather than dependent on system properties/parameters, which has immediate theoretical and physical ramifications. This is achieved by using time–varying feedback, leading to a non–autonomous system. For a comprehensive discussion on the merits of prescribed–time stabilization, we refer the reader to [37, Section 3.2]. Another important difference between our work and others (e.g., [17], where sliding mode control is used for finite–time boundary stabilization of the Schrödinger equation, or [11], where sliding mode control is used for the heat equation) is that the proposed feedback is *continuous*.

* Corresponding author.
E-mail address: dsteeves@ucsd.edu (D. Steeves).

https://doi.org/10.1016/j.ejcon.2020.02.009
0947-3580/

An application of the work to follow arises due to the connection of the Schrödinger equation to the Euler–Bernoulli beam equation [25], given by

$$w_{tt} + w_{xxxx} = 0 \tag{2}$$

and used to model the deflection of a beam due to applied loads. Indeed, by performing the change of variables $v = w_t - jw_{xx}$, one recovers (2) from (1). Exponential stabilization of thin beam/plate models have been studied extensively in the literature [24]. Seeking to stabilize these elastic systems in finite–time can be very desirable in structural dynamics which have strict performance requirements.

Perhaps the most recognized application of the Schrödinger equation is to model the wave function of a non–relativistic particle in quantum mechanical system. In these systems the appropriate model is (1) with interior control which is multiplied by the state, forming the *bilinear* Schrödinger equation [6,31] which is different than the *linearized* boundary–controlled version studied herein. In Section 8.2 we present a connection between boundary and interior distributed control of (1); while the bilinear structure is not exactly recovered, the analysis suggests a potential direction of research.

Recently, advances have been made to establish finite–time stabilization results for distributed–parameter systems [8,12,38]. In [8], the backstepping method is applied sequentially within the finite time domain to obtain a piecewise–continuous boundary controller which guarantees finite–time stabilization. This work's key idea differs from that in [37] in that, rather than rescaling the state, it uses a stabilizing reaction term which grows at every point in the sequence. This idea is extended in [12], where the stabilizing reaction term is scaled by a growing time–varying function. The authors of [12] leverage results from [8,36] to obtain an explicit and elegant representation for the control gain. This allows them to characterize the gain's growth–in–time, which allows them to guarantee prescribed–time stabilization under the assumption that the initial controller gain be chosen large enough.

1.1. Contributions

We utilize a time–varying, complex–valued backstepping transformation which necessitates a new study of the ensuing observer and controller gains. We develop new growth–in–time bounds for these gains by relying on their connection to their time–invariant counterparts. We utilize these bounds to develop an observer whose error converges to zero within the terminal time. Next, we demonstrate that the same results hold for the dual problem of stabilization via full–state feedback boundary control. Since the spectrum associated to the linearized Schrödinger equation consists of purely imaginary objects, we are not required to choose the initial observer and controller gains to be larger than some constant, as was the case in [12] for the reaction–diffusion equation. Finally, we combine these results to develop output feedback regulation under some modest assumptions on the choices of the initial controller and observer gains.

2. Estimation problem formulation

We study the linearized Schrödinger equation

$$v_t(x,t) = -jv_{xx}(x,t) \tag{3}$$

for $(x,t) \in (0,1) \times [t_0, t_0+T)$, where $T>0$, with initial condition $v_0(x) := v(x,t_0) \in H^2(0,1)$ and boundary conditions

$$v_x(0,t) = 0 \quad \text{and} \quad v(1,t) = u(t), \tag{4}$$

where $v(x,t)$ is the complex–valued state, j is the imaginary unit and $u(\cdot)$ is the controller. We study solutions of (3)–(4) in the space $v \in C^1([t_0,t_0+T); L^2(0,1)) \cap C^0([t_0,t_0+T); H^2(0,1))$ (cf. Section 8.1 for a discussion on well–posedness for a controller of interest).

The choices of boundary conditions in (4) correspond to the following ones for the Euler–Bernoulli beam equation: at $x=0$, the beam is permitted to slide, whereas at $x=1$, the beam is actuated through deflection and applied moment [35].

Suppose we have access to measurement quantity $v_x(1,t)$ at all times. For the Euler–Bernoulli beam problem, this choice of measurement is associated to measuring the beam's shear force and angle of deflection. We wish to estimate $v(x,t)$ for $x \in (0,1)$ such that our estimate error, denoted by $\tilde{v}(x,t)$, converges to zero within a *terminal* time which is prescribed independently of $v_0(x)$ and $\tilde{v}_0(x) := \tilde{v}_0(x,t_0)$.

While this work specializes to boundary conditions (4), we can also accommodate the boundary condition $v(0,t)=0$, which is the typical one used to describe the wave function of a *free* particle [31]. The necessary adaptations to the ensuing analysis are covered in [36, Rk. 2]. The case of interior distributed control/sensing is discussed in Section 8.2.

In this work, we assume the absences of measurement/model uncertainties and input disturbances. Let $\hat{v}(x,t)$ denote our estimate of $v(x,t)$; it follows that $\tilde{v}(x,t) = v(x,t) - \hat{v}(x,t)$. Replicating the design in [23, Section 5.1], we propose the observer

$$\hat{v}_t(x,t) = -j\hat{v}_{xx}(x,t) + p_1(x,t-t_0)\big[v_x(1,t) - \hat{v}_x(1,t)\big], \tag{5}$$

$$\hat{v}_x(0,t) = 0, \tag{6}$$

$$\hat{v}(1,t) = u(t), \tag{7}$$

which is a copy of the plant (3)–(4) with output measurement injection, and where $p_1(x,t-t_0)$ is the observer gain to be designed. The major difference between previous works (e.g., [10]) and this one is the time–dependence of $p_1(x,t-t_0)$, which we leverage to establish the more demanding prescribed–time estimation rather than exponential estimation.

The error equation associated to (3)–(4) and (5)–(7) is

$$\tilde{v}_t(x,t) = -j\tilde{v}_{xx}(x,t) - p_1(x,t-t_0)\tilde{v}_x(1,t), \tag{8}$$

$$\tilde{v}_x(0,t) = 0, \tag{9}$$

$$\tilde{v}(1,t) = 0. \tag{10}$$

Notice that for $p_1(x,t-t_0) \equiv 0$, (8)–(10) displays oscillatory behavior: every eigenvalue lies along the imaginary axis. The goal is to design $p_1(x,t-t_0)$ to eliminate these oscillations within the terminal time $T>t_0$ such that $\tilde{v}(x,t_0+T) \equiv 0$. We accomplish this by utilizing a Volterra–type backstepping transformation involving a time–varying kernel, giving rise to the time–dependence of $p_1(x,t-t_0)$.

2.1. Notation

For a complex-valued function $f(x,t) = u(x,t) + jv(x,t)$, we follow convention and denote its complex conjugate by $\overline{f(x,t)} := u(x,t) - jv(x,t)$, and its real and imaginary parts by $\mathrm{Re}\{f(x,t)\} := u(x,t)$ and $\mathrm{Im}\{f(x,t)\} := v(x,t)$, respectively. We denote its modulus by $|f(x,t)|^2 := f(x,t)\overline{f(x,t)}$.

3. Main results

Motivated by [37], we define two functions which are indispensable in the treatment to follow: for $t \in [t_0, t_0+T)$, let

$$\nu(t-t_0) := \left(1 - \frac{t-t_0}{T}\right), \tag{11}$$

Please cite this article as: D. Steeves, M. Krstic and R. Vazquez, Prescribed–time estimation and output regulation of the linearized Schrödinger equation by backstepping, European Journal of Control, https://doi.org/10.1016/j.ejcon.2020.02.009

and for $\tilde{\mu}_0 > 0$, let

$$\tilde{\mu}(t-t_0) := \frac{\tilde{\mu}_0}{\nu^2(t-t_0)}. \tag{12}$$

Notice that $\nu(0) = 1$ and decreases linearly to zero at $t = t_0 + T$. The power of $\nu(t-t_0)$ within the denominator of (12) is chosen as the smallest *integer* that is sufficiently large to guarantee the ensuing prescribed–time stabilization results. Larger powers within (12) can be considered, as was done in in [38] (for prescribed–time stabilization with *integer* power three) and [13] (kernel well–posedness for *arbitrary* power); choosing a larger power affects the trajectory of the prescribed–time stabilization (it causes the state estimate's approach to the true state to be more flat near the terminal time). However, achieving prescribed–time stabilization results for these larger powers is much more involved, and is still an open problem in most cases (see [13, Rk. 2] for details). We specialize to the case of denominator power of two.

We now present our first main result concerning the observation of (3)–(4).

Theorem 3.1. *Consider the observer (5)–(7) and let the time–varying observer gain be*

$$\begin{aligned} p_1(x,t-t_0) = {} & \frac{\sqrt{\tilde{\mu}_0}e^{\frac{-j(1-x^2)}{4T\nu(t-t_0)}}}{\nu(t-t_0)\sqrt{2(1-x^2)}} \\ & \times\left[(j-1)\mathrm{ber}_1\left(\sqrt{\tilde{\mu}(t-t_0)(1-x^2)}\right)\right. \\ & \left.-(1+j)\mathrm{bei}_1\left(\sqrt{\tilde{\mu}(t-t_0)(1-x^2)}\right)\right]. \end{aligned} \tag{13}$$

where $\mathrm{ber}_1(\cdot)$ *and* $\mathrm{bei}_1(\cdot)$ *are the Kelvin functions (see [1, Definition 9.9.1]). Then the observer error satisfies*

$$\|\tilde{v}(\cdot,t)\|_{L^2(0,1)} \le C_3\tilde{\mu}^{3/2}(t-t_0)e^{-\frac{\tilde{\mu}_0 T}{\nu(t-t_0)}}\|\tilde{v}_0(\cdot)\|_{L^2(0,1)}, \tag{14}$$

for $C_3 > 0$ *and for* $t \in [t_0, t_0+T)$. *In particular,*

$$\|\tilde{v}(\cdot,t)\|_{L^2(0,1)} \to 0 \quad \text{as} \quad t \to t_0+T. \tag{15}$$

We now consider the case where $u(t) = \mathcal{K}[v_x(1,t)](t-t_0)$ in (4). We present our second main result concerning output regulation of (3)–(4).

Theorem 3.2. *Suppose we select the time–varying boundary output feedback controller*

$$\begin{aligned} u(t) = {} & \frac{\sqrt{\mu_0}}{\nu(t-t_0)}\int_0^1 \frac{e^{\frac{j(1-y^2)}{4T\nu(t-t_0)}}}{\sqrt{2(1-y^2)}}\left[(j-1)\mathrm{ber}_1\left(\sqrt{\mu(t-t_0)(1-y^2)}\right)\right. \\ & \left.-(1+j)\mathrm{bei}_1\left(\sqrt{\mu(t-t_0)(1-y^2)}\right)\right]\hat{v}(y,t)dy, \end{aligned} \tag{16}$$

where $\hat{v}(x,t)$ *satisfies (5)–(7). Provided that one chooses*

$$\mu_0 > \left(\frac{4+\pi^2}{T\pi^2}\right)^2 \tag{17}$$

and

$$\tilde{\mu}_0 > \frac{\mu_0}{2}, \tag{18}$$

then

$$\|\hat{v}(\cdot,t)\|_{L^2(0,1)} + \|\tilde{v}(\cdot,t)\|_{L^2(0,1)} \to 0 \quad \text{as} \quad t \to t_0+T. \tag{19}$$

Moreover,

$$|u(t)| \to 0 \quad \text{as} \quad t \to t_0+T. \tag{20}$$

We now discuss advantages of the proposed output feedback (16). The feedback (16) is *explicit* and can be readily pre–computed, which is not the case for fixed–time optimal controllers with terminal constraints [32]. It is also *continuous*, which is not the case for sliding–mode controllers and can lead to undesirable effects [5]. The acquired stability due to (16) is prescribed by the user in a finite time which is *independent of the initial conditions*. Finally, the convergence that we establish (cf. (116)) has a *flatness* feature which implies that the state's convergence to zero be essentially flat near the terminal time; this in turn implies that subsequent time derivatives also be zero, and can be useful in application.

4. Backstepping design

We can view (3)–(4) formally as a heat equation with an imaginary diffusion coefficient. Motivated by [8,12,22], we apply the backstepping transformation

$$\tilde{v}(x,t) = \tilde{\psi}(x,t) - \int_x^1 p(x,y,t-t_0)\tilde{\psi}(y,t)dy, \tag{21}$$

to error Eqs. (8)–(10) and select the target error equation

$$\tilde{\psi}_t(x,t) = -j\tilde{\psi}_{xx}(x,t) - \tilde{\mu}(t-t_0)\tilde{\psi}(x,t), \tag{22}$$

$$\tilde{\psi}_x(0,t) = 0, \tag{23}$$

$$\tilde{\psi}(1,t) = 0. \tag{24}$$

Note that $\tilde{\mu}(t-t_0)$ applies unbounded positive damping to (22) as time approaches the terminal time.

The backstepping transformation (21) and our choice of target Eqs. (22)–(24) lead to the kernel equation

$$p_{xx} - p_{yy} = j(p_t - \tilde{\mu}(t-t_0)p), \tag{25}$$

$$p_x(0,y,t-t_0) = 0, \tag{26}$$

$$p(x,x,t-t_0) = -\frac{j\tilde{\mu}(t-t_0)x}{2}, \tag{27}$$

for $(x,y) \in \mathcal{T} := \{(x,y) \in (0,1)^2 \mid 0 \le x \le y \le 1\}$, provided that we choose our observer gain to be

$$p_1(x,t-t_0) = jp(x,1,t). \tag{28}$$

We propose the inverse transformation

$$\tilde{\psi}(x,t) = \tilde{v}(x,t) + \int_x^1 q(x,y,t-t_0)\tilde{v}(y,t)dy, \tag{29}$$

which, together with (22)–(24), lead to the inverse kernel equation

$$q_{xx} - q_{yy} = j(q_t + \tilde{\mu}(t-t_0)q), \tag{30}$$

$$q_x(0,y,t-t_0) = 0, \tag{31}$$

$$q(x,x,t-t_0) = -\frac{j\tilde{\mu}(t-t_0)x}{2}. \tag{32}$$

We now study the solutions to (25)–(27), (30)–(32) and derive several important properties.

5. Kernel solution and properties

Motivated be [36, Section 5], we perform the changes of variables

$$p(x,y,t-t_0) = -\frac{y}{2}e^{\int_{t_0}^t \tilde{\mu}(\tau-t_0)d\tau} f(z,t) \tag{33}$$

and $z = \sqrt{j(x^2-y^2)}$, which yield the PDE

$$f_t = f_{zz} + \frac{3}{z}f_z, \tag{34}$$

$$f_z(0,t) = 0, \tag{35}$$

$$f(0,t) = j\tilde{\mu}(t-t_0)e^{-\int_{t_0}^{t}\tilde{\mu}(\tau-t_0)d\tau}. \tag{36}$$

The solution to (34)–(36) is given in [30, Section 1.2.5] to be

$$f(z,t) = \sum_{n=0}^{\infty} \frac{z^{2n}}{4^n n!(n+1)!}\frac{d^n f(0,t)}{dt^n}. \tag{37}$$

In [12, Lemma 1], an explicit solution for (12), (36)–(37) is given (but with negative exponential power); this leads to

$$p(x,y,t-t_0) = -jy\tilde{\mu}(t-t_0)e^{\frac{-j(y^2-x^2)}{4Tv(t-t_0)}}\frac{I_1\left(\sqrt{j\tilde{\mu}(t-t_0)(y^2-x^2)}\right)}{\sqrt{j\tilde{\mu}(t-t_0)(y^2-x^2)}}. \tag{38}$$

Applying [1, Definition 9.9.1] yields

$$\begin{aligned} p(x,y,t-t_0) = y\sqrt{\frac{\tilde{\mu}(t-t_0)}{2(y^2-x^2)}}e^{\frac{-j(y^2-x^2)}{4Tv(t-t_0)}} \\ \times\left[(j-1)\mathrm{ber}_1\left(\sqrt{\tilde{\mu}(t-t_0)(y^2-x^2)}\right)\right. \\ \left. -(1+j)\mathrm{bei}_1\left(\sqrt{\tilde{\mu}(t-t_0)(y^2-x^2)}\right)\right]. \end{aligned} \tag{39}$$

For a fixed $\hat{t}\in[t_0,t_0+T)$ and $\hat{\mu} := \tilde{\mu}(\hat{t}-t_0)$, (38) can be written as

$$p(x,y,\hat{t}-t_0) = e^{\frac{-j(y^2-x^2)}{4Tv(\hat{t}-t_0)}}\hat{p}(x,y), \tag{40}$$

where $\hat{p}(x,y)$ satisfies

$$\hat{p}_{xx} - \hat{p}_{yy} = -j\hat{\mu}\hat{p}, \tag{41}$$

$$\hat{p}_x(0,y) = 0, \tag{42}$$

$$\hat{p}(x,x) = -\frac{j\hat{\mu}x}{2}. \tag{43}$$

We can repeat the same treatment to solve (30)–(32):

$$q(x,y,t-t_0) = -jy\tilde{\mu}(t-t_0)e^{\frac{-j(y^2-x^2)}{4Tv(t-t_0)}}\frac{J_1\left(\sqrt{j\tilde{\mu}(t-t_0)(y^2-x^2)}\right)}{\sqrt{j\tilde{\mu}(t-t_0)(y^2-x^2)}}, \tag{44}$$

or equivalently,

$$q(x,y,\hat{t}-t_0) = e^{\frac{-j(y^2-x^2)}{4Tv(\hat{t}-t_0)}}\hat{q}(x,y), \tag{45}$$

where $\hat{q}(x,y)$ satisfies

$$\hat{q}_{xx} - \hat{q}_{yy} = j\hat{\mu}\hat{q}, \tag{46}$$

$$\hat{q}_x(0,y) = 0, \tag{47}$$

$$\hat{q}(x,x) = -\frac{j\hat{\mu}x}{2}. \tag{48}$$

We utilize a method similar to that in [8, Lemma 2] to bound the H^1–norms of $\hat{p}(x,y)$ and $\hat{q}(x,y)$, which are *complex–valued*, in terms of $\hat{\mu}$. Our proof of the following result does not rely on any special properties of the Kelvin functions which form the solutions of $\hat{p}(x,y)$ and $\hat{q}(x,y)$. Instead, we generate estimates on $\hat{p}(x,y)$ and $\hat{q}(x,y)$ by utilizing Eqs. (41)–(43) and (46)–(48) directly.

Lemma 5.1. *The solution to (41)–(43) satisfies*

$$\|\hat{p}(\cdot,\cdot)\|^2_{H^1(\tilde{\mathcal{T}})} \le \frac{\hat{\mu}^2}{4}\left(\frac{\hat{\mu}}{12}+\frac{1}{2}+\frac{4}{\pi^2}\right), \tag{49}$$

and the solution to (46)–(48) satisfies

$$\|\hat{q}(\cdot,\cdot)\|^2_{H^1(\tilde{\mathcal{T}})} \le \frac{\hat{\mu}^2}{2}\left(\frac{\hat{\mu}}{3}+\frac{1}{2}+\frac{2}{\pi^2}\right)e^{\left(\frac{4}{\pi^2}+1\right)\sqrt{\hat{\mu}}}. \tag{50}$$

Proof. We multiply (41) by $\overline{\hat{p}_y(x,y)}$ and integrate with respect to x to obtain

$$\int_0^y \left(\hat{p}_{yy}\overline{\hat{p}_y} + \hat{p}_x\overline{\hat{p}_{xy}}\right)dx - \hat{p}_x(x,y)\overline{\hat{p}_y(x,y)}|_{x=0}^{y} = j\hat{\mu}\int_0^y \hat{p}\overline{\hat{p}_y}dx, \tag{51}$$

where we've employed Schwarz' theorem and the smoothness of $\hat{p}(x,y)$ (deduced from (38), (40)) to ensure the symmetry of mixed partial derivatives. Note that

$$\begin{aligned} \frac{\partial}{\partial y}|\hat{p}_y|^2 &= \hat{p}_{yy}\overline{\hat{p}_y} + \overline{\hat{p}_{yy}\hat{p}_y} \\ &= 2\mathrm{Re}\left\{\hat{p}_{yy}\overline{\hat{p}_y}\right\}, \end{aligned} \tag{52}$$

and similarly,

$$\frac{\partial}{\partial y}|\hat{p}_x|^2 = 2\mathrm{Re}\left\{\hat{p}_x\overline{\hat{p}_{xy}}\right\} \tag{53}$$

and

$$\frac{\partial}{\partial x}|\hat{p}|^2 = 2\mathrm{Re}\left\{\hat{p}\overline{\hat{p}_x}\right\}. \tag{54}$$

Furthermore, an application of the Cauchy–Riemann equations yields

$$\mathrm{Re}\left\{\hat{p}\overline{\hat{p}_x}\right\} = -\mathrm{Im}\left\{\hat{p}\overline{\hat{p}_y}\right\}. \tag{55}$$

Taking the real part of (51) and applying (52)–(55) yields

$$\int_0^y \frac{\partial}{\partial y}\left(|\hat{p}_y|^2+|\hat{p}_x|^2\right)dx - 2\mathrm{Re}\left\{\hat{p}_x(y,y)\overline{\hat{p}_y(y,y)}\right\} = \hat{\mu}\int_0^y \frac{\partial}{\partial x}|\hat{p}|^2dx. \tag{56}$$

By integrating the righthand side of (56) and applying (43), we obtain

$$\frac{d}{dy}\int_0^y \left(|\hat{p}_y|^2+|\hat{p}_x|^2\right)dx - \frac{\hat{\mu}^2}{4} = \hat{\mu}\left[\frac{\hat{\mu}^2y^2}{4} - |\hat{p}(0,y)|^2\right], \tag{57}$$

from which it follows that

$$\frac{d}{dy}\int_0^y \left(|\hat{p}_y|^2+|\hat{p}_x|^2\right)dx \le \frac{\hat{\mu}^2}{4}\left(1+\hat{\mu}y^2\right). \tag{58}$$

Integrating with respect to y yields

$$\int_0^1\int_0^y \left(|\hat{p}_y|^2+|\hat{p}_x|^2\right)dxdy \le \frac{\hat{\mu}^2}{4}\left(\frac{1}{2}+\frac{\hat{\mu}}{12}\right). \tag{59}$$

An application of Poincaré's inequality and integration by parts yields

$$\begin{aligned} \int_0^1\left(\int_0^y |\hat{p}|^2dx\right)dy &\le \frac{4}{\pi^2}\left(\int_0^1|\hat{p}(y,y)|^2dy + \int_0^1\int_0^y \frac{\partial}{\partial y}|\hat{p}|^2dxdy\right) \\ &= \frac{\hat{\mu}^2}{3\pi^2} + \frac{4}{\pi^2}\int_0^1\int_x^1\left(\hat{p}_y\overline{\hat{p}} + \hat{p}\overline{\hat{p}_y}\right)dydx \\ &= \frac{\hat{\mu}^2}{3\pi^2} + \frac{4}{\pi^2}\int_0^1\left(|\hat{p}(1,1)|^2 - |\hat{p}(x,x)|^2\right)dx \\ &= \frac{\hat{\mu}^2}{\pi^2}. \end{aligned} \tag{60}$$

Inequalities (59) and (60) together give (49).

The treatment for (50) is similar, except (56) is replaced with

$$\frac{d}{dy}\int_0^y \left(|\hat{q}_y|^2+|\hat{q}_x|^2\right)dx - \frac{\hat{\mu}^2}{4} = -\hat{\mu}\int_0^y \frac{\partial}{\partial x}|\hat{q}|^2dx. \tag{61}$$

We perform the change of variables $\check{y} = \sqrt{\hat{\mu}}y$ and $\check{q}(x,\check{y}) = \hat{q}(x,y)$. Notice that $\hat{q}_y(x,y) = \sqrt{\hat{\mu}}\check{q}_{\check{y}}(x,\check{y})$ and hence, after integrating, (61) rewrites as

$$\int_0^{\check{y}}\left(|\check{q}_{\check{y}}|^2+\hat{\mu}^{-1}|\check{q}_x|^2\right)dx - \frac{\sqrt{\hat{\mu}}\check{y}}{4} = -\int_0^{\check{y}}\int_0^s \frac{\partial}{\partial x}|\check{q}(x,s)|^2dxds. \tag{62}$$

Please cite this article as: D. Steeves, M. Krstic and R. Vazquez, Prescribed–time estimation and output regulation of the linearized Schrödinger equation by backstepping, European Journal of Control, https://doi.org/10.1016/j.ejcon.2020.02.009

Evaluating the righthand side of (62) yields

$$\begin{aligned}&\int_0^{\check{y}} \left(|\check{q}_{\check{y}}|^2 + \hat{\mu}^{-1}|\check{q}_x|^2\right)dx \\ &\leq \frac{\sqrt{\hat{\mu}}\check{y}}{4} + \int_0^{\check{y}} |\check{q}(0,s)|^2 ds \\ &\leq \frac{\sqrt{\hat{\mu}}\check{y}}{2}\left(\frac{1}{2} + \frac{\check{y}^2}{3}\right) + \left(\frac{4}{\pi^2}+1\right)\int_0^{\check{y}}\int_0^s |\check{q}_s(x,s)|^2 dx ds. \end{aligned} \tag{63}$$

where we've employed [23, Lemmas 2.1, 2.4] and the Cauchy–Riemann equations. Defining $V_1(\check{y}) := \int_0^{\check{y}} \left(|\check{q}_{\check{y}}|^2 + \hat{\mu}^{-1}|\check{q}_x|^2\right)dx$ and using the fact that $0 \leq \check{y} \leq \sqrt{\hat{\mu}}$, we obtain

$$V_1(\check{y}) \leq \frac{\hat{\mu}}{2}\left(\frac{\hat{\mu}}{3}+\frac{1}{2}\right) + \left(\frac{4}{\pi^2}+1\right)\int_0^{\sqrt{\hat{\mu}}} V_1(\check{y})d\check{y}. \tag{64}$$

An application of Grönwall's inequality yields

$$V_1(\check{y}) \leq \frac{\hat{\mu}}{2}\left(\frac{\hat{\mu}}{3}+\frac{1}{2}\right)e^{\left(\frac{4}{\pi^2}+1\right)\sqrt{\hat{\mu}}}. \tag{65}$$

We return to the original variables and integrate to obtain

$$\int_0^1\int_0^y \left(|\hat{q}_y|^2 + |\hat{q}_x|^2\right)dxdy \leq \frac{\hat{\mu}^2}{2}\left(\frac{\hat{\mu}}{3}+\frac{1}{2}\right)e^{\left(\frac{4}{\pi^2}+1\right)\sqrt{\hat{\mu}}}, \tag{66}$$

which, together with an argument identical to that for (60), establishes (50). □

Remark 5.2. Lemma 5.1 differs from [8, Lemma 2] in that (41) and (46) contain terms scaled by the imaginary unit, which effectively causes a rotation in the complex plane as seen in (55). For example, one could view (41) as a set of coupled equations, where the new states are the real and imaginary parts of the original states. Furthermore, the constant within the exponential of (50) is explicitly recovered, which will be important in Section 8.

We now relate the bounds obtained in Lemma 5.1 to their time–varying counterparts.

Corollary 5.3. *The solution to (25)–(27) satisfies*

$$\|p(\cdot,\cdot,t-t_0)\|_{H^1(\check{\mathcal{T}})} \leq C_1\tilde{\mu}^{3/2}(t-t_0), \tag{67}$$

for $C_1 := \sqrt{\frac{1}{48} + \frac{1}{8\tilde{\mu}_0} + \frac{1}{\pi^2\tilde{\mu}_0}}$, *and the solution to (30)–(32) satisfies*

$$\|q(\cdot,\cdot,t-t_0)\|_{H^1(\check{\mathcal{T}})} \leq C_2\tilde{\mu}^{3/2}(t-t_0)e^{\left(\frac{2}{\pi^2}+\frac{1}{2}\right)\sqrt{\tilde{\mu}(t-t_0)}}, \tag{68}$$

for $C_2 := \sqrt{\frac{1}{6} + \frac{1}{4\tilde{\mu}_0} + \frac{1}{\pi^2\tilde{\mu}_0}}$.

The proof follows directly from Lemma 5.1 and (40), (45).

6. Prescribed–time stabilization of estimate error

We first demonstrate the utility of choosing target Eqs. (22)–(24) in the following result.

Lemma 6.1. *The solution to (22)–(24) satisfies*

$$\|\tilde{\psi}(\cdot,t)\|_{L^2(0,1)} = e^{-\frac{\tilde{\mu}_0 T}{\nu(t-t_0)}}\|\tilde{\psi}_0(\cdot)\|_{L^2(0,1)}. \tag{69}$$

Proof. Define

$$V_2(\psi) := \frac{1}{2}\int_0^1 |\tilde{\psi}(x,t)|^2 dx. \tag{70}$$

The derivative of V_2 along the trajectory of (22) is given by

$$\begin{aligned}\dot{V}_2 &= \frac{1}{2}\int_0^1 \left[\tilde{\psi}_t(x,t)\overline{\tilde{\psi}(x,t)} + \tilde{\psi}(x,t)\overline{\tilde{\psi}_t(x,t)}\right]dx \\ &= -2\tilde{\mu}(t-t_0)V_2 + \frac{j}{2}\int_0^1 \left[\overline{\tilde{\psi}_{xx}(x,t)\overline{\tilde{\psi}(x,t)}} - \tilde{\psi}_{xx}(x,t)\overline{\tilde{\psi}(x,t)}\right]dx \\ &= -2\tilde{\mu}(t-t_0)V_2 + \int_0^1 \mathrm{Im}\left\{\tilde{\psi}_{xx}(x,t)\overline{\tilde{\psi}(x,t)}\right\}dx, \end{aligned} \tag{71}$$

since for a complex–valued function $\alpha(x,t)$,

$$\frac{j}{2}\left[\overline{\alpha(x,t)} - \alpha(x,t)\right] = \mathrm{Im}\{\alpha(x,t)\}.$$

Integrating by parts and applying (23)–(24) reveals

$$\begin{aligned}&\int_0^1 \mathrm{Im}\left\{\tilde{\psi}_{xx}(x,t)\overline{\tilde{\psi}(x,t)}\right\}dx \\ &= \int_0^1 \left(\mathrm{Im}\{\tilde{\psi}_{xx}\}\mathrm{Re}\{\tilde{\psi}\} - \mathrm{Re}\{\tilde{\psi}_{xx}\}\mathrm{Im}\{\tilde{\psi}\}\right)dx \\ &= 0; \end{aligned} \tag{72}$$

the result follows from (12) and (71)–(72). □

We can now establish Theorem 3.1.

Proof of Theorem 3.1. We begin by relating stability result (69) to the observer error Eqs. (8)–(10). Note that by applying the triangle and Cauchy–Schwarz inequalities to (21), we obtain

$$\|\tilde{v}(\cdot,t)\|_{L^2(0,1)} \leq \left(1 + \|p(\cdot,\cdot,t-t_0)\|_{H^1(\check{\mathcal{T}})}\right)\|\tilde{\psi}(\cdot,t)\|_{L^2(0,1)}. \tag{73}$$

Repeating the same treatment for (29), we obtain

$$\|\tilde{\psi}(\cdot,t)\|_{L^2(0,1)} \leq \left(1 + \|q(\cdot,\cdot,t-t_0)\|_{H^1(\check{\mathcal{T}})}\right)\|\tilde{v}(\cdot,t)\|_{L^2(0,1)}. \tag{74}$$

We apply (67) and (69) to (73) to obtain

$$\|\tilde{v}(\cdot,t)\|_{L^2(0,1)} \leq \left(1 + C_1\mu^{3/2}(t-t_0)\right)e^{-\frac{\tilde{\mu}_0 T}{\nu(t-t_0)}}\|\tilde{\psi}_0(\cdot)\|_{L^2(0,1)}. \tag{75}$$

We evaluate (74) at $t = t_0$, employ (50) and apply the result to (75) to obtain

$$\|\tilde{v}(\cdot,t)\|_{L^2(0,1)} \leq C_3\mu^{3/2}(t-t_0)e^{-\frac{\tilde{\mu}_0 T}{\nu(t-t_0)}}\|\tilde{v}_0(\cdot)\|_{L^2(0,1)}, \tag{76}$$

for $C_3 := (1 + C_2\tilde{\mu}_0^{3/2}e^{\left(\frac{2}{\pi^2}+\frac{1}{2}\right)\sqrt{\tilde{\mu}_0}})(\frac{1}{\tilde{\mu}_0^{3/2}} + C_1)$. Claim (15) follows from the definitions of (11), (12). □

7. Dual result

Next, we study the prescribed–time stabilization of (3)–(4), where we select $u(t) = \mathcal{K}[v(\cdot,t)](t-t_0)$ to be a full–state boundary controller in feedback form. We employ the backstepping transformation

$$\psi(x,t) = v(x,t) - \int_0^x k(x,y,t-t_0)v(y,t)dy, \tag{77}$$

and we select the target equation

$$\psi_t(x,t) = -j\psi_{xx}(x,t) - \mu(t-t_0)\psi(x,t), \tag{78}$$

$$\psi_x(0,t) = 0, \tag{79}$$

$$\psi(1,t) = 0 \tag{80}$$

for

$$\mu(t-t_0) := \frac{\mu_0}{\nu^2(t-t_0)}, \tag{81}$$

where $\mu_0 > 0$. These choices lead to the kernel equations

$$k_{xx} - k_{yy} = j(k_t + \mu(t-t_0)k), \tag{82}$$

Please cite this article as: D. Steeves, M. Krstic and R. Vazquez, Prescribed–time estimation and output regulation of the linearized Schrödinger equation by backstepping, European Journal of Control, https://doi.org/10.1016/j.ejcon.2020.02.009

$$k_y(x,0,t-t_0)=0, \tag{83}$$

$$k(x,x,t-t_0)=-\frac{j\mu(t-t_0)x}{2}, \tag{84}$$

for $(x,y)\in\mathcal{T}:=\{(x,y)\in(0,1)^2\mid 0\le y\le x\le 1\}$. Comparing (82)–(84) to (30)–(32), and after taking into the account the difference between $\tilde{\mathcal{T}}$ and $\mathcal{T}$, it follows that

$$\begin{aligned}k(x,y,t-t_0)=x\sqrt{\frac{\mu(t-t_0)}{2(x^2-y^2)}}e^{\frac{j(x^2-y^2)}{4T\nu(t-t_0)}}\\ \times\left[(j-1)\mathrm{ber}_1\left(\sqrt{\mu(t-t_0)(x^2-y^2)}\right)\right.\\ \left.-(1+j)\mathrm{bei}_1\left(\sqrt{\mu(t-t_0)(x^2-y^2)}\right)\right].\end{aligned} \tag{85}$$

From (77) and (85), we recover the full–state feedback controller

$$\begin{aligned}u_{\text{state}}(t)=\frac{\sqrt{\mu_0}}{\nu(t-t_0)}\int_0^1\frac{e^{\frac{j(1-y^2)}{4T\nu(t-t_0)}}}{\sqrt{2(1-y^2)}}\\ \times\left[(j-1)\mathrm{ber}_1\left(\sqrt{\mu(t-t_0)(1-y^2)}\right)\right.\\ \left.-(1+j)\mathrm{bei}_1\left(\sqrt{\mu(t-t_0)(1-y^2)}\right)\right]v(y,t)dy.\end{aligned} \tag{86}$$

To recover the inverse of transformation (77), one need only follow a similar method that was used to recover (44), yielding transformation

$$v(x,t)=\psi(x,t)+\int_0^x l(x,y,t-t_0)\psi(y,t)dy, \tag{87}$$

with

$$l(x,y,t-t_0)=jx\mu(t-t_0)e^{\frac{j(x^2-y^2)}{4T\nu(t-t_0)}}\frac{J_1\left(\sqrt{j\mu(t-t_0)(x^2-y^2)}\right)}{\sqrt{j\mu(t-t_0)(x^2-y^2)}}. \tag{88}$$

We obtain the following result.

Proposition 7.1. *Consider the linearized Schrödinger Eqs. (3)–(4). Implementing the boundary controller (86) yields*

$$\|v(\cdot,t)\|_{L^2(0,1)}\le C_3\mu^{3/2}(t-t_0)e^{-\frac{\mu_0 T}{\nu(t-t_0)}}\|v_0(\cdot)\|^2_{L^2(0,1)}, \tag{89}$$

for $t\in[t_0,t_0+T)$, and in particular,

$$\|v(\cdot,t)\|_{L^2(0,1)}\to 0\quad\text{as}\quad t\to t_0+T. \tag{90}$$

Furthermore,

$$|u_{\text{state}}(t)|\to 0\quad\text{as}\quad t\to t_0+T. \tag{91}$$

Proof. Employing a similar technique as used in Section 5, we can show that

$$\|k(\cdot,\cdot,t-t_0)\|_{H^1(\mathcal{T})}\le C_2\mu^{3/2}(t-t_0)e^{\left(\frac{2}{\pi^2}+\frac{1}{2}\right)\sqrt{\mu(t-t_0)}} \tag{92}$$

and

$$\|l(\cdot,\cdot,t-t_0)\|_{H^1(\mathcal{T})}\le C_1\mu^{3/2}(t-t_0). \tag{93}$$

Notice that Lemma (6.1) also holds for (78)–(80), that is,

$$\|\psi(\cdot,t)\|_{L^2(0,1)}=e^{-\frac{\mu_0 T}{\nu(t-t_0)}}\|\psi_0(\cdot)\|_{L^2(0,1)}. \tag{94}$$

Applying the triangle and Cauchy–Schwarz inequalities to (77), we obtain

$$\|\psi(\cdot,t)\|_{L^2(0,1)}\le\left(1+\|k(\cdot,\cdot,t-t_0)\|_{H^1(\mathcal{T})}\right)\|v(\cdot,t)\|_{L^2(0,1)}; \tag{95}$$

repeating this treatment for (87) gives

$$\|v(\cdot,t)\|_{L^2(0,1)}\le\left(1+\|l(\cdot,\cdot,t-t_0)\|_{H^1(\mathcal{T})}\right)\|\psi(\cdot,t)\|_{L^2(0,1)}. \tag{96}$$

Applying (94) to (96) and then (95) at $t=t_0$ to the resulting inequality, and utilizing (92), (93) yields

$$\|v(\cdot,t)\|_{L^2(0,1)}\le C_3\mu^{3/2}(t-t_0)e^{-\frac{\mu_0 T}{\nu(t-t_0)}}\|v_0(\cdot)\|^2_{L^2(0,1)}. \tag{97}$$

Evaluating (87) at $x=1$ and applying [23, Lemma 2.4] gives

$$|u_{\text{state}}(t)|\le C\mu^k(t-t_0)e^{-\frac{\mu_0 T}{\nu(t-t_0)}}\to 0\quad\text{as}\quad t\to t_0+T, \tag{98}$$

for C, $k>0$, since the decaying exponential component dominates the righthand side of (98) as $t\to t_0+T$. □

We now combine the results of Theorem 3.1 and Proposition 7.1 to demonstrate the claims in Theorem 3.2.

8. Output feedback

We now select the controller

$$u(t)=\int_0^1 k(1,y,t-t_0)\hat{v}(y,t)dy, \tag{99}$$

which can be rewritten as $u(t)=u_{\text{state}}(t)-\tilde{u}(t)$, where

$$\tilde{u}(t):=\int_0^1 k(1,y,t-t_0)\tilde{v}(y,t)dy. \tag{100}$$

We establish Theorem 3.2.

Proof of Theorem 3.2. Studying the stability of the system (3)–(4), (99) is equivalent to studying the stability of the $(\hat{v},\tilde{v})$ system. We will accomplish the latter by first studying the $(\hat{\psi},\tilde{\psi})$ target system, where the equation governing $\hat{\psi}$ is obtained via the same transformations (77), (87) but replacing v,ψ with $\hat{v},\hat{\psi}$. We obtain the cascade system

$$\begin{aligned}\hat{\psi}_t=&-j\hat{\psi}_{xx}-\mu(t-t_0)\hat{\psi}+\left[p_1(x,t-t_0)\right.\\ &\left.-\int_0^x k(x,y,t-t_0)p_1(y,t-t_0)dy\right]\tilde{\psi}_x(1,t),\end{aligned} \tag{101}$$

$$\tilde{\psi}_t=-j\tilde{\psi}_{xx}-\tilde{\mu}(t-t_0)\tilde{\psi}, \tag{102}$$

$$\hat{\psi}_x(0,t)=\hat{\psi}(1,t)=0, \tag{103}$$

$$\tilde{\psi}_x(0,t)=\tilde{\psi}(1,t)=0. \tag{104}$$

Let

$$V_3(\hat{\psi},\tilde{\psi}):=\frac{1}{2}\int_0^1\left[|\hat{\psi}|^2+|\tilde{\psi}|^2\right]dx. \tag{105}$$

Differentiating V_3 along the trajectory of (101)–(104) gives

$$\begin{aligned}\dot{V}_3=&-\mu(t-t_0)\int_0^1|\hat{\psi}|^2dx-\tilde{\mu}(t-t_0)\int_0^1|\tilde{\psi}|^2dx\\ &+\int_0^1\mathrm{Re}\left\{p_1(x,t-t_0)\tilde{\psi}_x(1,t)\overline{\hat{\psi}}(x,t)\right\}dx\\ &-\int_0^1\mathrm{Re}\left\{\left(\int_0^x k(x,y,t-t_0)p_1(y,t-t_0)dy\tilde{\psi}_x(1,t)\right)\overline{\hat{\psi}}(x,t)\right\}dx.\end{aligned} \tag{106}$$

Please cite this article as: D. Steeves, M. Krstic and R. Vazquez, Prescribed–time estimation and output regulation of the linearized Schrödinger equation by backstepping, European Journal of Control, https://doi.org/10.1016/j.ejcon.2020.02.009

Separating the real and imaginary parts within the last two terms of (106) and applying Young's inequality yields

$$\begin{aligned}\dot{V}_3 \leq & -\left(\mu(t-t_0)-\frac{1}{a}\right)\int_0^1 |\hat{\psi}|^2dx-\tilde{\mu}(t-t_0)\int_0^1|\tilde{\psi}|^2dx\\ &+a\int_0^1\left|p_1(x,t-t_0)\tilde{\psi}_x(1,t)\right|^2dx\\ &+a\int_0^1\left|\left(\int_0^x k(x,y,t-t_0)p_1(y,t-t_0)dy\right)\tilde{\psi}_x(1,t)\right|^2dx\end{aligned} \tag{107}$$

for $a>\frac{1}{\mu_0}$. Now define

$$V_4(\tilde{\psi}):=\frac{1}{2}\int_0^1|\tilde{\psi}_{xx}|^2dx; \tag{108}$$

differentiating along the trajectory of (102), (104) yields

$$\begin{aligned}\dot{V}_4=&\frac{1}{2}\int_0^1\left[-j\tilde{\psi}_{xxxx}-\tilde{\mu}(t-t_0)\tilde{\psi}_{xx}\right]\overline{\tilde{\psi}_{xx}}dx\\ &+\frac{1}{2}\int_0^1\left[j\overline{\tilde{\psi}_{xxxx}}-\tilde{\mu}(t-t_0)\overline{\tilde{\psi}_{xx}}\right]\tilde{\psi}_{xx}dx\\ =&-2\tilde{\mu}(t-t_0)V_4+\frac{j}{2}\left[-\tilde{\psi}_{xxx}\overline{\tilde{\psi}_{xx}}|_{x=0}^1+\tilde{\psi}_{xx}\overline{\tilde{\psi}_{xxx}}|_{x=0}^1\right].\end{aligned} \tag{109}$$

Assume $\tilde{\psi}(\cdot,t)\in C(0,1)$ for $t\in[t_0,t_0+T)$ (this is ensured, for example, if $\tilde{\psi}_0(x)\in H_0^1(0,1)$ – see [14, Section 7.1] for details). Then it follows by evaluating (102) at $x=1$ that $\tilde{\psi}_{xx}(1,t)\equiv 0$; similarly, it follows by differentiating (102) and evaluating at $x=0$ that $\tilde{\psi}_{xxx}(0,t)\equiv 0$. Hence,

$$\dot{V}_4=-2\tilde{\mu}(t-t_0)V_4, \tag{110}$$

and thus,

$$\|\tilde{\psi}_{xx}(\cdot,t)\|_{L^2(0,1)}=e^{-\frac{\tilde{\mu}_0 T}{\nu(t-t_0)}}\|\tilde{\psi}_{xx}(\cdot,t_0)\|_{L^2(0,1)}. \tag{111}$$

It follows by applications of Cauchy-Schwarz and [23, Lemmas 2.1, 2.4] that

$$\begin{aligned}\dot{V}_3\leq & -\frac{\min\left\{\mu_0-\frac{1}{a},\tilde{\mu}_0\right\}}{\nu^2(t-t_0)}V_3+aC_4\|p(\cdot,\cdot,t-t_0)\|_{H^1(\mathcal{T})}^2\\ &\times\|k(\cdot,\cdot,t-t_0)\|_{H^1(\mathcal{T})}^2e^{-\frac{2\tilde{\mu}_0T}{\nu(t-t_0)}}\|\tilde{\psi}_{xx}(\cdot,t_0)\|_{L^2(0,1)}^2,\end{aligned} \tag{112}$$

for $C_4>0$. Applying the comparison lemma, (67), (92) and evaluating the resulting integral yields

$$\begin{aligned}V_3(t)\leq & aC_4(\mu_0\tilde{\mu}_0)^3(C_1C_2\|\tilde{\psi}_{xx}(\cdot,t_0)\|_{L^2(0,1)})^2\\ &\times\int_{t_0}^t\frac{e^{\frac{\left(\frac{4}{\pi^2}+1\right)\sqrt{\mu_0}-2\tilde{\mu}_0T}{\nu(s-t_0)}}e^{-\int_s^t\frac{\min\left\{\mu_0-\frac{1}{a},\tilde{\mu}_0\right\}}{\nu(\eta-t_0)}d\eta}}{\nu^{12}(s-t_0)}ds\\ &+e^{-\frac{\min\left\{\mu_0-\frac{1}{a},\tilde{\mu}_0\right\}T}{\nu(t-t_0)}+\min\left\{\mu_0-\frac{1}{a},\tilde{\mu}_0\right\}T}V_3(t_0)\\ \leq & aC_4(\mu_0\tilde{\mu}_0)^3(C_1C_2\|\tilde{\psi}_{xx}(\cdot,t_0)\|_{L^2(0,1)})^2\\ &\times e^{-\frac{\min\left\{\mu_0-\frac{1}{a},\tilde{\mu}_0\right\}T}{\nu(t-t_0)}}\int_{t_0}^t\frac{e^{\frac{\left(\frac{4}{\pi^2}+1\right)\sqrt{\mu_0}-\tilde{\mu}_0T}{\nu(s-t_0)}}e^{\frac{\min\left\{\mu_0-\frac{1}{a},\tilde{\mu}_0\right\}T-\tilde{\mu}_0T}{\nu(s-t_0)}}}{\nu^{12}(s-t_0)}ds\\ &+e^{-\frac{\min\left\{\mu_0-\frac{1}{a},\tilde{\mu}_0\right\}T}{\nu(t-t_0)}+\min\left\{\mu_0-\frac{1}{a},\tilde{\mu}_0\right\}T}V_3(t_0)\\ \leq & aCe^{-\frac{\left(\min\left\{\mu_0-\frac{1}{a},\tilde{\mu}_0\right\}+\tilde{\mu}_0\right)T-\left(\frac{4}{\pi^2}+1\right)\sqrt{\mu_0}}{\nu(t-t_0)}}\sum_{n=0}^{10}\left(\frac{b_n}{\nu(t-t_0)}\right)^nV_3(t_0),\end{aligned} \tag{113}$$

for C, $b_n>0$. Applying (29), (68) and (77), (92) at $t=t_0$ to the righthand side of (113) yields

$$\begin{aligned}&\|\hat{\psi}(\cdot,t)\|_{L^2(0,1)}^2+\|\tilde{\psi}(\cdot,t)\|_{L^2(0,1)}^2\\ &\leq\frac{aC}{\nu^{10}(t-t_0)}e^{-\frac{\left(\min\left\{\mu_0-\frac{1}{a},\tilde{\mu}_0\right\}+\tilde{\mu}_0\right)T-\left(\frac{4}{\pi^2}+1\right)\sqrt{\mu_0}}{\nu(t-t_0)}}\\ &\quad\times\left(\|\hat{v}_0(\cdot)\|_{L^2(0,1)}^2+\|\tilde{v}_0(\cdot)\|_{L^2(0,1)}^2\right).\end{aligned} \tag{114}$$

Furthermore, employing (21), (67) and (87), (93) yields

$$\begin{aligned}&\|\hat{v}(\cdot,t)\|_{L^2(0,1)}^2+\|\tilde{v}(\cdot,t)\|_{L^2(0,1)}^2\\ &\leq\left(1+C_1\mu^{3/2}(t-t_0)\right)^2\left(\|\hat{\psi}(\cdot,t)\|_{L^2(0,1)}^2+\|\tilde{\psi}(\cdot,t)\|_{L^2(0,1)}^2\right).\end{aligned} \tag{115}$$

From (114) and (115), it follows that

$$\begin{aligned}&\|\hat{v}(\cdot,t)\|_{L^2(0,1)}^2+\|\tilde{v}(\cdot,t)\|_{L^2(0,1)}^2\\ &\leq\frac{aC}{\nu^{16}(t-t_0)}e^{-\frac{\left(\min\left\{\mu_0-\frac{1}{a},\tilde{\mu}_0\right\}+\tilde{\mu}_0\right)T-\left(\frac{4}{\pi^2}+1\right)\sqrt{\mu_0}}{\nu(t-t_0)}}\\ &\quad\times\left(\|\hat{v}_0(\cdot)\|_{L^2(0,1)}^2+\|\tilde{v}_0(\cdot)\|_{L^2(0,1)}^2\right).\end{aligned} \tag{116}$$

Suppose $\tilde{\mu}_0\geq\mu_0$; since the decaying exponential component dominates the righthand side of (116) as $t\to t_0+T$, it suffices to choose μ_0 satisfying (17) to guarantee that (116) converges to zero as $t\to t_0+T$. Now suppose $\tilde{\mu}_0<\mu_0$; then one can choose $\frac{1}{\mu_0}<a<\frac{1}{\mu_0-\tilde{\mu}_0}$ so that $\min\{\mu_0-\frac{1}{a},\tilde{\mu}_0\}=\tilde{\mu}_0$. Hence, we must restrict our choice of $\tilde{\mu}_0$ to satisfy

$$\left(\frac{4+\pi^2}{\pi^2}\right)\frac{\sqrt{\mu_0}}{2T}<\tilde{\mu}_0 \tag{117}$$

to guarantee that (116) converges to zero as $t\to t_0+T$. Furthermore, by utilizing (92) and (100), is it straightforward to show that choice (18) also suffices to ensure

$$|\tilde{u}(t)|\to 0\qquad\text{as}\qquad t\to t_0+T. \tag{118}$$

Hence, (118) together with (98) guarantees (20). This finishes the proof. □

Notice from (13) and (16) that the parameters μ_0 and $\tilde{\mu}_0$ define the controller and observer *initial gains*, respectively. In (17) and (18), we require that they not be designed independently, and hence the controller and observer cannot immediately be designed separately. A main topic in [38] is to design similar observer and controller kernels to (38) and (85) such that *certainty equivalence* holds for an equation related to (3). The corresponding analysis, which depends on the power of $\nu(t-t_0)$ within the blow–up function (12), is involved and is not presented in this work. However, similar steps to those appearing in [38] can be performed to separately design the controller (16) and the observer (5)–(7) with (13).

8.1. Well–posedness of closed–loop system

While the well–posedness of a similar closed–loop system to the one presented here was studied in [22] using a semigroup method, our reliance on time–varying blow–up functions (12) and (81), which appear in our target system (101)–(104), demands a different approach.

We first demonstrate the well–posedness of the target system (101)–(104) and then leverage the boundedness of the transformations (29), (87) for times $t\in[t_0,t_0+\bar{T}]$ for any positive $\bar{T}<T$. Since boundedness is valid until *(but not including)* the terminal time t_0+T, the well–posedness result we provide is only valid up to times arbitrarily close to t_0+T.

Please cite this article as: D. Steeves, M. Krstic and R. Vazquez, Prescribed–time estimation and output regulation of the linearized Schrödinger equation by backstepping, European Journal of Control, https://doi.org/10.1016/j.ejcon.2020.02.009

By performing the change of variables

$$\tilde{\psi}_I(x,t) := \tilde{\psi}(x,t)e^{\int_{t_0}^{t}\tilde{\mu}(\tau-t_0)d\tau},$$

one recovers a simplified version of (102), (104) whose well–posedness was studied in [22, Theorem 3.1] by using a Riesz basis approach with the Lumer–Phillips result to obtain the solution

$$\tilde{\psi}_I \in C^1([t_0, t_0+\bar{T}]; L^2(0,1)) \cap C^0([t_0, t_0+\bar{T}]; H^2(0,1))$$

provided that $\tilde{\psi}_I(\cdot, t_0) \in H^2(0,1)$. One can perform a similar change of variables

$$\hat{\psi}_I(x,t) := \hat{\psi}(x,t)e^{\int_{t_0}^{t}\mu(\tau-t_0)d\tau}$$

for (101), (103) and then invoke [22, Theorem 4.1] to obtain

$$\hat{\psi}_I \in C^1([t_0, t_0+\bar{T}]; L^2(0,1)) \cap C^0([t_0, t_0+\bar{T}]; H^2(0,1))$$

provided that $\hat{\psi}_I(\cdot, t_0) \in H^2(0,1)$. It follows from the bounded invertibility of (29), (87) and the above changes of variables that (3)–(4), (16) is well–posed with solution

$$v \in C^1([t_0, t_0+\bar{T}]; L^2(0,1)) \cap C^0([t_0, t_0+\bar{T}]; H^2(0,1)),$$

provided that $v_0(x) \in H^2(0,1)$ and it be compatible with (4) (i.e., $v_{0,x}(0) = 0$ and $v_0(1) = u(0)$).

The above analysis covers most applications where prescribed–time stabilization is required: for example, in tactical missile guidance, where not only the solution but also the system cease to exist at the terminal time, and thus well–posedness beyond this time is unnecessary. For other applications where the system continues to exist past time T (e.g., the Euler–Bernoulli beam), the control law implementation discussed in Section 9.1 allows one to extend the solution *in practice*.

Remark 8.1. The above mathematical analysis does not hold for $t \geq t_0 + T$ due to the unbounded damping term in (101); for these times, mathematical well–posedness of (3)–(4), (16) remains an open problem.

8.2. Connections to interior distributed control and observation

The above results present a *boundary* controller and observer that yield prescribed–time stabilization of (3)–(4). We now form a connection between these results and ones for interior distributed control and observation, that is, where the controller and output measurements appear within the domain of the equations. Our treatment follows that of [2, Theorem 2.2].

Consider the control problem given by

$$v_t = -jv_{xx} + \mathbb{1}_\omega u(x,t), \tag{119}$$

$$v_x(0,t) = 0, \tag{120}$$

$$v(1,t) = 0, \tag{121}$$

for $(x,t) \in (0,1) \times [t_0, t_0+T)$, where $\mathbb{1}_\omega$ denotes a smooth indicator function with support in an open set $\omega \subset (0,1)$; the goal is to establish prescribed–time stabilization by designing the controller $u(x,t)$ appropriately.

For demonstration purposes, we take $t_0 = 0$ and $\omega = \left(\frac{1}{4}, \frac{3}{4}\right)$. We define the sets $\Omega := (0,1)$, $\breve{\omega} := \left(\frac{3}{8}, \frac{5}{8}\right)$ (we require $\bar{\breve{\omega}} \subset \omega$, where for any set κ, $\bar{\kappa}$ denotes its closure) and $\breve{\Omega} := \Omega \setminus \bar{\breve{\omega}} = \left(0, \frac{3}{8}\right) \cup \left(\frac{5}{8}, 1\right)$. We will show that the control problem (119)–(121) can be solved by Proposition 7.1 for (3)–(4) for particular choice of $u(x,t)$.

Let α satisfy the boundary controlled Schrödinger Eq. (3) on the domain $(x,t) \in \breve{\Omega} \times [t_0, t_0+T)$, where we now actuate with controllers $\breve{u}_1$ and $\breve{u}_2$ at the boundaries

$$\alpha\left(\frac{3}{8}, t\right) = \breve{u}_1(t) \qquad \text{and} \qquad \alpha\left(\frac{5}{8}, t\right) = \breve{u}_2(t),$$

and where we impose the boundary conditions

$$\alpha_x(0,t) = 0 \qquad \text{and} \qquad \alpha_x(1,t) = 0.$$

Hence, we allow α to evolve on two disjoint components of Ω, where each component is actuated at its inner boundary. We select $\breve{u}_1$ similarly to (86) but adapt it for the domain $\left(0, \frac{3}{8}\right)$ to obtain

$$\begin{aligned}\breve{u}_1(t) = \frac{\sqrt{\mu_0}}{\nu(t-t_0)} \int_0^a \frac{e^{\frac{j\left(a^2-y^2\right)}{4\nu(t-t_0)}}}{\sqrt{2(a^2-y^2)}} \\ \times \left[(j-1)\mathrm{ber}_1\left(\sqrt{\mu(t-t_0)\left(a^2-y^2\right)}\right)\right. \\ \left. -(1+j)\mathrm{bei}_1\left(\sqrt{\mu(t-t_0)\left(a^2-y^2\right)}\right)\right]\alpha(y,t)dy\end{aligned} \tag{122}$$

for $a = \frac{3}{8}$. Notice from (3)–(4) that by performing the change of variables $\breve{x} := 1 - x$ and $\breve{\alpha}(\breve{x}, t) = \alpha(x,t)$ on the connected component $\left(\frac{5}{8}, 1\right)$ of $\breve{\Omega}$, $\breve{\alpha}$ is equivalent to its counterpart on $\left(0, \frac{3}{8}\right)$ and hence we select $\breve{u}_2$ in the same way. Proposition 7.1 now directly applies to α on each connected component.

In addition, let β satisfy (119)–(121) with $u(x,t) \equiv 0$ (that is, β is the solution to the *uncontrolled* Schrödinger equation).

Following the methodology of [15, Theorem 8.18], define the mollifier

$$g(x) := \begin{cases} e^{-\frac{1}{x}}, & x > 0 \\ 0, & x \leq 0 \end{cases}$$

and the convolutions $h_1, h_2 \colon [0,1] \to [0,1]$ given by

$$h_1(x) := \frac{\int_{\frac{1}{4}}^{x} g\left(s-\frac{1}{4}\right)g\left(\frac{3}{8}-s\right)ds}{\int_{\frac{1}{4}}^{\frac{3}{8}} g\left(s-\frac{1}{4}\right)g\left(\frac{3}{8}-s\right)ds},$$

$$h_2(x) := \frac{\int_{\frac{5}{8}}^{x} g\left(s-\frac{5}{8}\right)g\left(\frac{3}{4}-s\right)ds}{\int_{\frac{5}{8}}^{\frac{3}{4}} g\left(s-\frac{5}{8}\right)g\left(\frac{3}{4}-s\right)ds}.$$

We now define a smoothed square function $\theta \colon [0,1] \to [0,1]$ as

$$\theta(x) := (1 - h_1(x)) + h_2(x).$$

It follows that $\theta(x) = 1$ for $x \in \left[0, \frac{1}{4}\right] \cup \left[\frac{3}{4}, 1\right]$, $\theta(x) = 0$ for $x \in \left[\frac{3}{8}, \frac{5}{8}\right]$, and that $\theta \in C^\infty(0,1)$. Finally, define the convolution $h_3 \colon [0,T] \to [0,1]$ as

$$h_3(t) := \frac{\int_{\frac{T}{4}}^{t} g\left(s-\frac{T}{4}\right)g\left(\frac{3T}{4}-s\right)ds}{\int_{\frac{T}{4}}^{\frac{3T}{4}} g\left(s-\frac{T}{4}\right)g\left(\frac{3T}{4}-s\right)ds}$$

and the smoothed step function $\eta \colon [0,T] \to [0,1]$ as

$$\eta(t) := 1 - h_3(t). \tag{123}$$

It follows that $\eta(t) = 1$ for $t \in \left[0, \frac{T}{4}\right]$, $\eta(t) = 0$ for $t \in \left[\frac{3T}{4}, T\right]$, and $\eta \in C^\infty(0,T)$. By choosing the interior distributed controller

$$\mathbb{1}_\omega u(x,t) = j\left[\theta''(\alpha - \eta\beta) + 2\theta'(\alpha_x - \eta\beta_x)\right] + (1-\theta)\eta'\beta, \tag{124}$$

it is straightforward to show that

$$v := \theta\alpha + (1-\theta)\eta\beta \tag{125}$$

verifies (119)–(121) with $\|v(\cdot,t)\|_{L^2(0,1)} \to 0$ as $t \to T$ due to Proposition 7.1 and (123). Hence, Proposition 7.1 can be extended to ensure prescribed–time stabilization by means of the interior distributed control (124). However, one *cannot* use (125) to write (124) in the form

$$\mathbb{1}_\omega \mathcal{K}[v(\cdot,t)](t)$$

for some operator $\mathcal{K}$ without dependence on α, β or their derivatives: these *virtual states* are summed in (125) within $\breve{\Omega} \cap \omega \neq \emptyset$,

Please cite this article as: D. Steeves, M. Krstic and R. Vazquez, Prescribed–time estimation and output regulation of the linearized Schrödinger equation by backstepping, European Journal of Control, https://doi.org/10.1016/j.ejcon.2020.02.009

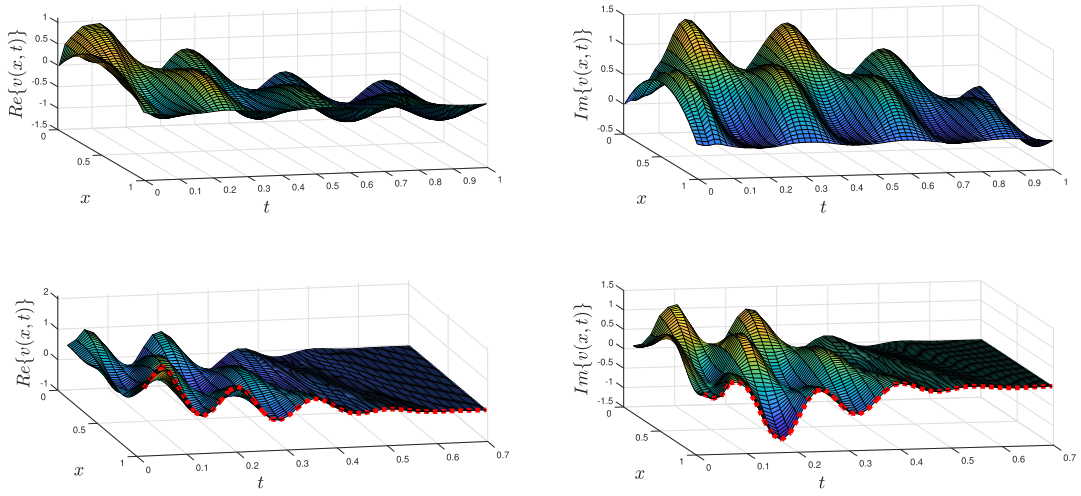

Fig. 1. The real and imaginary parts of the open–loop (top) and closed–loop output feedback (bottom) responses of (3)–(4). The real and imaginary parts of the controller (99) appear at the boundary of the bottom surface plots and are identified by the dotted lines.

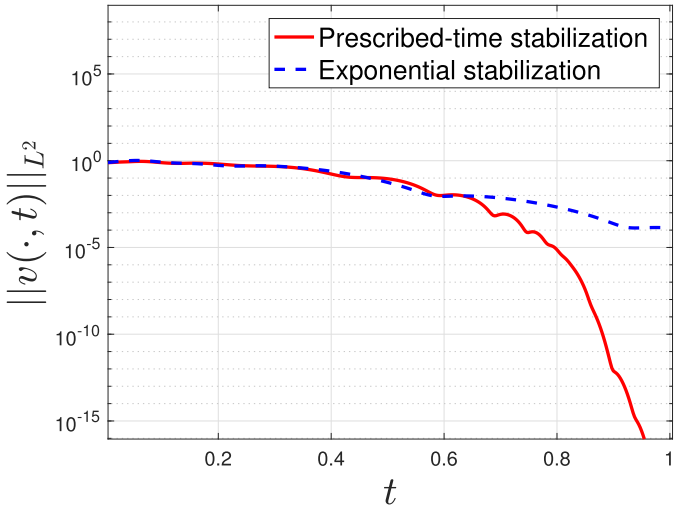

Fig. 2. Logarithmic plot of the energy of the closed–loop output feedback system (3)–(4), (13), (16) compared to that proposed in [22].

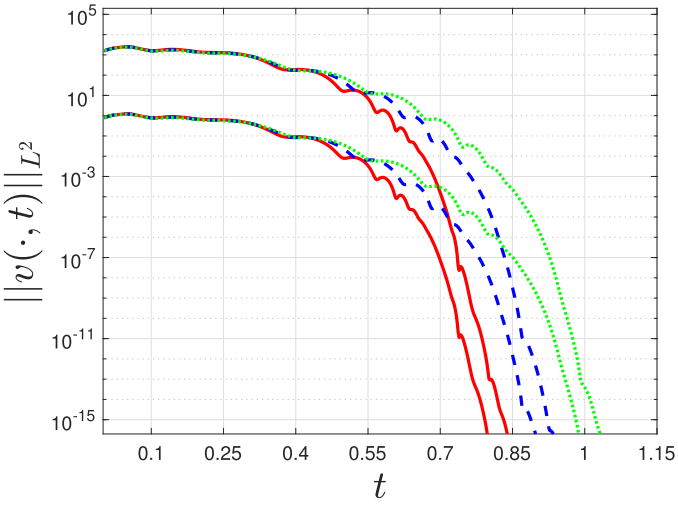

Fig. 3. Logarithmic plot of the energy of the closed–loop output feedback system (3)–(4), (13), (16) for terminal times $T = 0.85$ (solid line), $T = 1$ (dashed line) and $T = 1.15$ (dotted line) with initial conditions $v_0(x) = 3(1+j)x(1-x)$ (lower initial energy) and $v_0(x) = 1000(1+2j)\sin(\pi x)$ (higher initial energy).

and since β evolves according to an uncontrolled equation and by the product rule, additional terms in (124) are needed for cancellation in (119). Hence, the above does not imply that interior stabilization of the *bilinear* Schrödinger equation can be recovered by boundary stabilization of its linearized version. For rapid (exponential) stabilization of the linearized bilinear Schrödinger equation, see [7].

Using the same techniques, we can develop a state observer which utilizes interior measurements and ensures prescribed–time stabilization of its error equation. The resulting error equation resembles

$$\tilde{v}_t = -j\tilde{v}_{xx} + \mathbb{1}_\omega(p(x,t)\tilde{v}_x + g(x,t)), \tag{126}$$

$$\tilde{v}_x(0,t) = 0, \tag{127}$$

$$\tilde{v}(1,t) = 0, \tag{128}$$

where the *virtual state* terms required for cancellation are gathered within $g(x,\ t)$. Let $\tilde{\alpha}$ solve the error Eqs. (8)–(10) on the domain $(x,t) \in \breve{\Omega} \times [t_0, t_0+T)$, but now with two output measurement injections at $x = \frac{3}{8}$ (with associated gain $p_1(x,\ t)$, defined on $\left(0, \frac{3}{8}\right) \times [0,T)$) and $x = \frac{5}{8}$ (with associated gain $p_2(x,\ t)$, defined on $\left(\frac{5}{8}, 1\right) \times [0,T)$). Let $\tilde{\beta}$ satisfy (8)–(10) but excluding output measurement injection. By choosing

$$\mathbb{1}_\omega p(x,t)\tilde{v}_x = \theta\left[p_1(x,t)\tilde{v}_x\left(\frac{3}{8},t\right) + p_2(x,t)\tilde{v}_x\left(\frac{5}{8},t\right)\right]$$

one can verify that

$$\tilde{v} = \theta\tilde{\alpha} + (1-\theta)\eta\tilde{\beta}$$

solves (126)–(128) with appropriate choice of $g(x,\ t)$ to ensure cancellations. Furthermore, by Theorem 3.1 and (123), $\|\tilde{v}(\cdot,t)\|_{L^2} \to 0$ as $t \to T$.

It is clear that the interior distributed controllers and observers established above by their boundary counterparts are suboptimal in design since they rely only on controlling/sensing at two distinct points in $\partial\breve{\omega} \subset \omega$ rather than the entirety of ω. An interesting potential direction of future research is to apply the above method in succession to take advantage of the full control/sensing domain of authority ω.

Please cite this article as: D. Steeves, M. Krstic and R. Vazquez, Prescribed–time estimation and output regulation of the linearized Schrödinger equation by backstepping, European Journal of Control, https://doi.org/10.1016/j.ejcon.2020.02.009

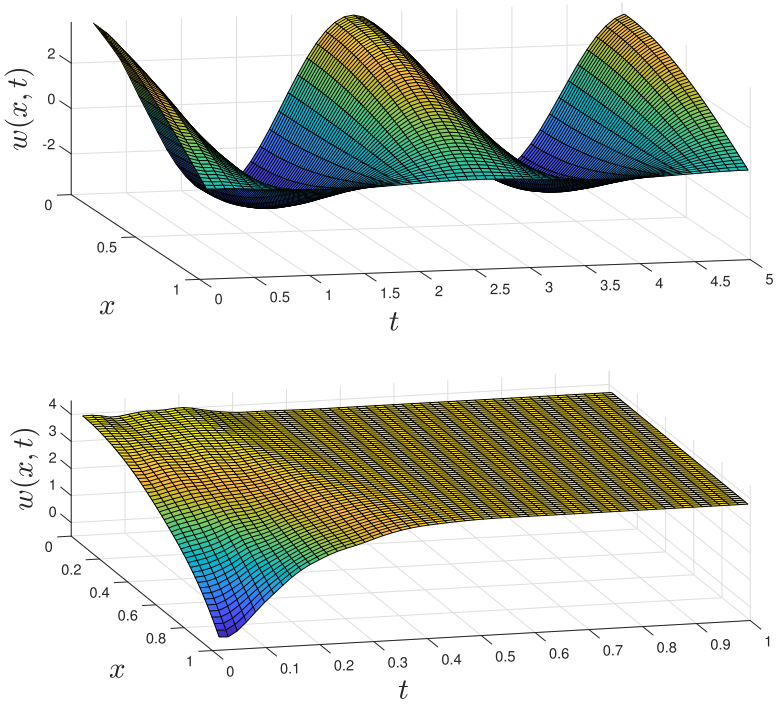

Fig. 4. The open–loop (top) and closed–loop output feedback (bottom) responses of (2). The beam is stabilized to a constant profile within the terminal time.

9. Simulation study

We present the results of a simulation of the closed–loop system (3)–(4), (5)–(7) with observer gain (13) and boundary controller (16) in Figs. 1–2. The simulation was generated using the *implicit Euler method*, where the initial conditions were chosen to be $v_0(x) = 3(1+j)x(1-x)$ and $\hat{v}_0(x) \equiv 0$, the initial controller and observer gains were chosen to be $\mu_0 = \tilde{\mu}_0 = 13$, and the terminal time was assigned to be $T = 1$. In Fig. 1, surface plots of the real parts of the open– and closed–loop responses of (3)–(4) are shown. The top surface plot demonstrates the undamped oscillations of the open–loop system. The bottom surface plot shows the suppression of these oscillations by the time–varying output feedback regulation.

Fig. 2 compares the L^2 energies of the closed–loop output feedback system derived herein (which guarantees prescribed–time stabilization) and that which is proposed in [22] (which guarantees exponential stabilization). We saturate the controller and observer gains given in (13) and (16) at $t = 0.85$, which due to machine precision, is sufficient to simulate $v(\cdot, t_0 + T) \equiv 0$.

Fig. 3 demonstrates that the closed–loop system is stabilized independently of initial conditions: we provide the results of simulations where both the initial conditions and the stabilization time are varied.

As discussed in Sections 1 and 2, the relation between (2) and (3) is given by

$$v = w_t - jw_{xx}. \tag{129}$$

Hence, one can utilize the output feedback controller developed herein to stabilize the Euler–Bernoulli beam *to a constant profile* within the terminal time (see [35] for more details). The particular beam we study is one which is allowed to slide at $x = 0$ and is actuated at $x = 1$: this is realized by the boundary conditions $w_x(0,t) = w_{xxx}(0,t) = 0$, $w(1,t) = u_1(t)$ and $w_{xx}(1,t) = u_2(t)$, where $u_1(t)$ and $u_2(t)$ are controls. By comparing (4) to (129), one notices that $u_1(t)$ is given by integrating the real part of (16), whereas $u_2(t)$ is given as the negative imaginary part of (16). Due to the integration required to recover $u_1(t)$, we only achieve prescribed–time stabilization to a constant profile. We present the results of a simulation of (2) in Fig. 4, where we've used the same numerical methods as above and with initial conditions $((w(x,0), w_t(x,0)) = (-4(x^2-1), 0)$.

9.1. Practical implementation

Regardless of the boundedness of the input (20), the controller gain diverging at the terminal time can present some issues in implementation. Computing the feedback necessitates the inner product between vectors with very large and very small magnitude, which may present numerical problems (e.g., machine precision). This high–gain challenge is not particular to our approach: it is present in all fixed–time stabilizations results (e.g., in sliding–mode control, the discontinuous control with high gain can manifest as *chattering* behavior near the sliding surface or excitation of high–frequency dynamics in flexible structures, and is also present in finite–horizon optimal control with a terminal constraint).

To address this problem, one could instead require the state to converge to a small neighborhood around zero (imposing the limitation of machine precision), and utilize the time–invariant controller in [22] (which can be designed to have small gain) thereafter. This implementation prevents the controller gain from diverging, and moreover, allows mathematical well–posedness to be extended past T. The same implementation method can be employed to ensure that the observer gain remain bounded.

10. Conclusion and future work

We have presented *explicit* and *continuous* boundary controllers and observers that ensure stabilization of the linearized Schrödinger equation and observer error equation within a terminal time prescribed *independently of the initial conditions*. We have demonstrated that our results can be used in conjunction for output feedback regulation while conserving the prescribed–time stabilization property under modest assumptions on the initial controller and observer gains.

Please cite this article as: D. Steeves, M. Krstic and R. Vazquez, Prescribed–time estimation and output regulation of the linearized Schrödinger equation by backstepping, European Journal of Control, https://doi.org/10.1016/j.ejcon.2020.02.009

We have recalled that the linearized Schrödinger equation is connected to the Euler–Bernoulli beam equation, and we've demonstrated that our results can be used to stabilize this beam to a constant profile in within the terminal time. The methods used in [35] (which ensure exponential stabilization of the beam) cannot be replicated to recover prescribed–time stabilization of the beam *to the zero profile* due to the time dependence of the kernels within the backstepping transformations. Further research is required to fill this gap.

Absent from our presentation was robustness analysis for the proposed closed–loop system. A partial robustness result is reported in [8, Rk. 7] and [12, Section 3] for incorporating an additional term $\tilde{\delta}(t)v$ in (3), where $\tilde{\delta}(t)$ is an uncertain but bounded function; this robustness extends to the above treatment if (16) is implemented with $\hat{v} \equiv v$ (i.e., for full–state feedback). Robustness to other model uncertainties, controller and measurement noise require several highly involved analyses due to the time–varying gains employed herein. We aspire to address some of these questions in future works.

Acknowledgement

This work was partially supported by the Air Force Office of Scientific Research under the Award No.: FA9550-18-1-0105.

Declaration of Competing Interest

The authors declare that there are no conflicts of interest in submitting this work. They certify that they have no affiliations with or involvement in any organization or entity with any financial interests in the subject matter or materials discussed in this manuscript. Some of the preliminary results within our submission for the full-state feedback controller have been accepted for presentation at the 2020 American Control Conference. This EJC submission is significantly different than the ACC submission, focusing instead on the estimation problem, and alike insofar as the control result is combined with the estimation result herein to generate output feedback after some important technical verifications.

References

[1] M. Abramowitz, I.A. Stegun, Handbook of Mathematical Functions: with Formulas, Graphs, and Mathematical Tables, 55, Courier Corporation, 1965.
[2] F. Ammar-Khodja, A. Benabdallah, M. González Burgos, L. de Teresa, Recent results on the controllability of linear coupled parabolic problems: a survey, Math. Control Relat. Fields 1 (3) (2011) 267–306.
[3] V. Andrieu, L. Praly, A. Astolfi, Homogeneous approximation, recursive observer design, and output feedback, SIAM J. Control Optim. 47 (4) (2008) 1814–1850.
[4] K. Beauchard, J.M. Coron, M. Mirrahimi, P. Rouchon, Implicit Lyapunov control of finite dimensional Schrödinger equations, Syst. Control Lett. 56 (5) (2007) 388–395.
[5] S.P. Bhat, D.S. Bernstein, Finite-time stability of continuous autonomous systems, SIAM J. Control Optim. 38 (3) (2000) 751–766.
[6] U. Boscain, T. Chambrion, M. Sigalotti, On some open questions in bilinear quantum control, in: Proceedings of the European Control Conference (ECC), IEEE, 2013, pp. 2080–2085.
[7] J.-M. Coron, L. Gagnon, M. Morancey, Rapid stabilization of a linearized bilinear 1-d Schrödinger equation, J. Mathématiques Pures et Appliquées 115 (2018) 24–73.
[8] J.-M. Coron, H.-M. Nguyen, Null controllability and finite time stabilization for the heat equations with variable coefficients in space in one dimension via backstepping approach, Arch. Ration. Mech. Anal. 225 (3) (2017) 993–1023.
[9] E. Cruz-Zavala, J.A. Moreno, L.M. Fridman, Uniform robust exact differentiator, IEEE Trans. Autom. Control 56 (11) (2011) 2727–2733.
[10] J. Deutscher, S. Kerschbaum, Backstepping control of coupled linear parabolic pides with spatially varying coefficients, IEEE Trans. Autom. Control 63 (12) (2018) 4218–4233.
[11] S. Drakunov, E. Barbieri, D. Silver, Sliding mode control of a heat equation with application to arc welding, in: Proceeding of the IEEE International Conference on Control Applications IEEE International Conference on Control Applications held together with IEEE International Symposium on Intelligent Contro, IEEE, 1996, pp. 668–672.
[12] N. Espitia, A. Polyakov, D. Efimov, W. Perruquetti, Boundary time–varying feedbacks for fixed-time stabilization of constant-parameter reaction–diffusion systems, Automatica 103 (2019) 398–407.
[13] N. Espitia, A. Polyakov, D. Efimov, W. Perruquetti, Some characterizations of boundary time–varying feedbacks for fixed–time stabilization of reaction–diffusion systems, in: Proceeding of the Control of Systems Governed by Partial Differential Equations (CPDE), IFAC, 2019, pp. 165–170.
[14] L.C. Evans, Partial Differential Equations, American Mathematical Society, 1998.
[15] G.B. Folland, Real Analysis: Modern Techniques and their Applications, John Wiley & Sons, 2013.
[16] L. Fraguela, M.T. Angulo, J.A. Moreno, L. Fridman, Design of a prescribed convergence time uniform robust exact observer in the presence of measurement noise, in: Proceeding of the IEEE 51st IEEE Conference on Decision and Control (CDC), IEEE, 2012, pp. 6615–6620.
[17] B.-Z. Guo, J.-J. Liu, Sliding mode control and active disturbance rejection control to the stabilization of one-dimensional Schrödinger equation subject to boundary control matched disturbance, Int. J. Robust Nonlinear Control 24 (16) (2014) 2194–2212.
[18] V.T. Haimo, Finite time controllers, SIAM J. Control Optim. 24 (4) (1986) 760–770.
[19] X. Huang, W. Lin, B. Yang, Global finite-time stabilization of a class of uncertain nonlinear systems, Automatica 41 (5) (2005) 881–888.
[20] E. Jiménez-Rodríguez, A.J. Muñoz-Vázquez, J.D. Sánchez-Torres, A.G. Loukianov, A note on predefined-time stability, IFAC-PapersOnLine 51 (13) (2018) 520–525.
[21] E. Jiménez-Rodríguez, J.D. Sánchez-Torres, A.G. Loukianov, On optimal predefined-time stabilization, Int. J. Robust Nonlinear Control 27 (17) (2017) 3620–3642.
[22] M. Krstic, B.-Z. Guo, A. Smyshlyaev, Boundary controllers and observers for the linearized Schrödinger equation, SIAM J. Control Optim. 49 (4) (2011) 1479–1497.
[23] M. Krstic, A. Smyshlyaev, Boundary Control of PDEs: A Course on backstepping Designs, 16, SIAM, 2008.
[24] J.E. Lagnese, Boundary Stabilization of thin Plates, SIAM, 1989.
[25] E. Machtyngier, E. Zuazua, Stabilization of the schrodinger equation, Portugaliae Mathematica 51 (2) (1994) 243–256.
[26] A. Polyakov, Nonlinear feedback design for fixed-time stabilization of linear control systems, IEEE Trans. Autom. Control 57 (8) (2011) 2106–2110.
[27] A. Polyakov, D. Efimov, W. Perruquetti, Finite-time and fixed-time stabilization: Implicit Lyapunov function approach, Automatica 51 (2015) 332–340.
[28] A. Polyakov, L. Fridman, Stability notions and Lyapunov functions for sliding mode control systems, J. Frankl. Inst. 351 (4) (2014) 1831–1865.
[29] A. Polyakov, A. Poznyak, Lyapunov function design for finite–time convergence analysis:"twisting" controller for second-order sliding mode realization, Automatica 45 (2) (2009) 444–448.
[30] A.D. Polyanin, V.E. Nazaikinskii, Handbook of Linear Partial Differential Equations for Engineers and Scientists, Chapman and Hall/CRC, 2015.
[31] P. Rouchon, Control of a quantum particle in a moving potential well, IFAC Proc. Vol. 36 (2) (2003) 287–290.
[32] E. Ryan, Finite-time stabilization of uncertain nonlinear planar systems, Dyn. Control 1 (1) (1991) 83–94.
[33] J.D. Sánchez-Torres, E.N. Sanchez, A.G. Loukianov, Predefined-time stability of dynamical systems with sliding modes, in: Proceedings of the American Control Conference (ACC), IEEE, 2015, pp. 5842–5846.
[34] O.J. Smith, Posicast control of damped oscillatory systems, Proc. IRE 45 (9) (1957) 1249–1255.
[35] A. Smyshlyaev, B.-Z. Guo, M. Krstic, Arbitrary decay rate for euler-bernoulli beam by backstepping boundary feedback, IEEE Trans. Autom. Control 54 (5) (2009) 1134–1140.
[36] A. Smyshlyaev, M. Krstic, On control design for pdes with space-dependent diffusivity or time-dependent reactivity, Automatica 41 (9) (2005) 1601–1608.
[37] Y. Song, Y. Wang, J. Holloway, M. Krstic, Time–varying feedback for regulation of normal–form nonlinear systems in prescribed finite time, Automatica 83 (2017) 243–251.
[38] D. Steeves, M. Krstic, R. Vazquez, Prescribed–time H^1–stabilization of reaction–diffusion equations by means of output feedback, in: Proceedings of the European Control Conference (ECC), IEEE, 2019, pp. 1932–1937.

Please cite this article as: D. Steeves, M. Krstic and R. Vazquez, Prescribed–time estimation and output regulation of the linearized Schrödinger equation by backstepping, European Journal of Control, https://doi.org/10.1016/j.ejcon.2020.02.009